TECTONICS, VOL. 28, TC2003, doi:10.1029/2007TC002251, 2009

Slow subduction of a thick ultrahigh-pressure terrane

Andrew R. C. Kylander-Clark,[1] Bradley R. Hacker,[1] Clark M. Johnson,[2] Brian L. Beard,[2] and Nancy J. Mahlen[2]

Received 18 December 2007; revised 6 October 2008; accepted 15 December 2008; published 10 March 2009.

[1] High-precision Lu-Hf and Sm-Nd ages reported here cover a large portion of the Western Gneiss Region (WGR) ultrahigh-pressure (UHP) terrane, Norway, and range from 413.9 ± 3.7 to 397.1 ± 4.8 Ma. Collectively, new and existing geochronologic data for eclogites demonstrate that eclogite facies metamorphism occurred over a large area (60,000 km^2) for an unexpectedly long period of >20 Ma. A thermal model using slow subduction (2–4 mm a^{-1}) of a relatively warm and thick slab can reproduce the observed *P-T-t* history of the WGR UHP terrane, indicating that large UHP terranes with protracted peak or near-peak histories probably reflect slow subduction of relatively thick crustal sections.

Citation: Kylander-Clark, A. R. C., B. R. Hacker, C. M. Johnson, B. L. Beard, and N. J. Mahlen (2009), Slow subduction of a thick ultrahigh-pressure terrane, *Tectonics*, *28*, TC2003, doi:10.1029/2007TC002251.

1. Introduction

[2] The number of recognized ultrahigh-pressure (UHP) rocks worldwide has increased dramatically in the last two decades, and as such, awareness of their importance in processes such as orogenesis, the generation and rearrangement of continental crust, and interaction between the crust and the mantle has grown. Significant advances have been made toward understanding the evolution of UHP terranes, but some fundamental processes remain enigmatic, particularly their rates and mechanisms of formation.

[3] UHP terranes are distinguished by the presence of coesite, and the best studied UHP terranes appear to have formed by subduction to depths of 100–135 km [*Chopin et al.*, 1991; *Schertl et al.*, 1991; *Carswell et al.*, 1997; *Reinecke*, 1998; *Cuthbert et al.*, 2000; *Masago*, 2000; *Ota et al.*, 2000; *Carswell and Cuthbert*, 2003; *Hirajima and Nakamura*, 2003; *Krogh Ravn and Terry*, 2004]. With rare exceptions, UHP rocks show peak temperatures of 600–800°C [*Hacker*, 2006]. These observations have led to the paradigm that UHP terranes were not heated to higher temperatures because they were rapidly subducted, experience peak *P-T* conditions for a short time [e.g., *Carswell et al.*, 2003b; *Zheng et al.*, 2003], and were then rapidly exhumed and cooled [e.g., *Eide et al.*, 1994; *Rubatto and Hermann*, 2001; *Hacker et al.*, 2003; *Root et al.*, 2005; *Parrish et al.*, 2006]. Geochronologic studies suggest that some UHP terranes, indeed, spent only a few million years at HP conditions [e.g., *Leech et al.*, 2005]. However, other UHP terranes in eastern China [*Hacker et al.*, 2006; *Liu et al.*, 2006a], western China [*Mattinson et al.*, 2006], and Greenland [*McClelland et al.*, 2006] were held at high-pressure depths for 15–20 Ma. The first two of these are so-called giant UHP terranes (more that a few thousand square kilometers), which might well have evolved over a more protracted period than smaller UHP terranes.

[4] Geochronologic studies also show that some UHP terranes underwent rapid near-isothermal decompression, followed by rapid cooling [*Maruyama and Parkinson*, 2000; *Liu et al.*, 2006b; *Parrish et al.*, 2006; *Hacker*, 2007]. The need for rapid cooling has led to a second paradigm, that UHP terranes are thin (<10 km [e.g., *Ernst*, 2006]), although field relations and thermal models have been used to argue that some UHP terranes are thick [*Hacker et al.*, 2000; *Root et al.*, 2005].

[5] In this paper we present new Sm-Nd and Lu-Hf ages that bolster earlier indications [*Kylander-Clark et al.*, 2007] of a 20-Ma duration for (U)HP metamorphism in western Norway. We then use simple thermal models to assess the tectonic settings under which protracted prograde metamorphism, followed by rapid exhumation and cooling, is possible. These results bear on questions such as the following: What dimensions can a UHP body have if it is to cool fast enough to retain HP mineral assemblages and yield the temperature-time curves observed in UHP terranes? What subduction velocities are possible? What changes in subduction behavior are permissible?

2. Geologic Background

[6] The WGR consists chiefly of tonalitic to granodioritic Baltica gneiss, called the Western Gneiss Complex (WGC), which is overlain by a stack of oceanic and continental allochthons (Figure 1). The allochthons are principally 1700–950 Ma [*Corfu*, 1980; *Schärer*, 1980; *Tucker et al.*, 1990; *Root et al.*, 2005] and were emplaced eastward over the WGC during the Scandian Orogeny at ~435–400 Ma [*Roberts and Gee*, 1985; *Hacker and Gans*, 2005]. It was during this orogeny that the signature UHP metamorphism of the Western Gneiss Region developed at *P-T* conditions

[1]Department of Earth Science, University of California, Santa Barbara, California, USA.
[2]Department of Geology and Geophysics, University of Wisconsin-Madison, Madison, Wisconsin, USA.

0278-7407/09/2007TC002251$12.00

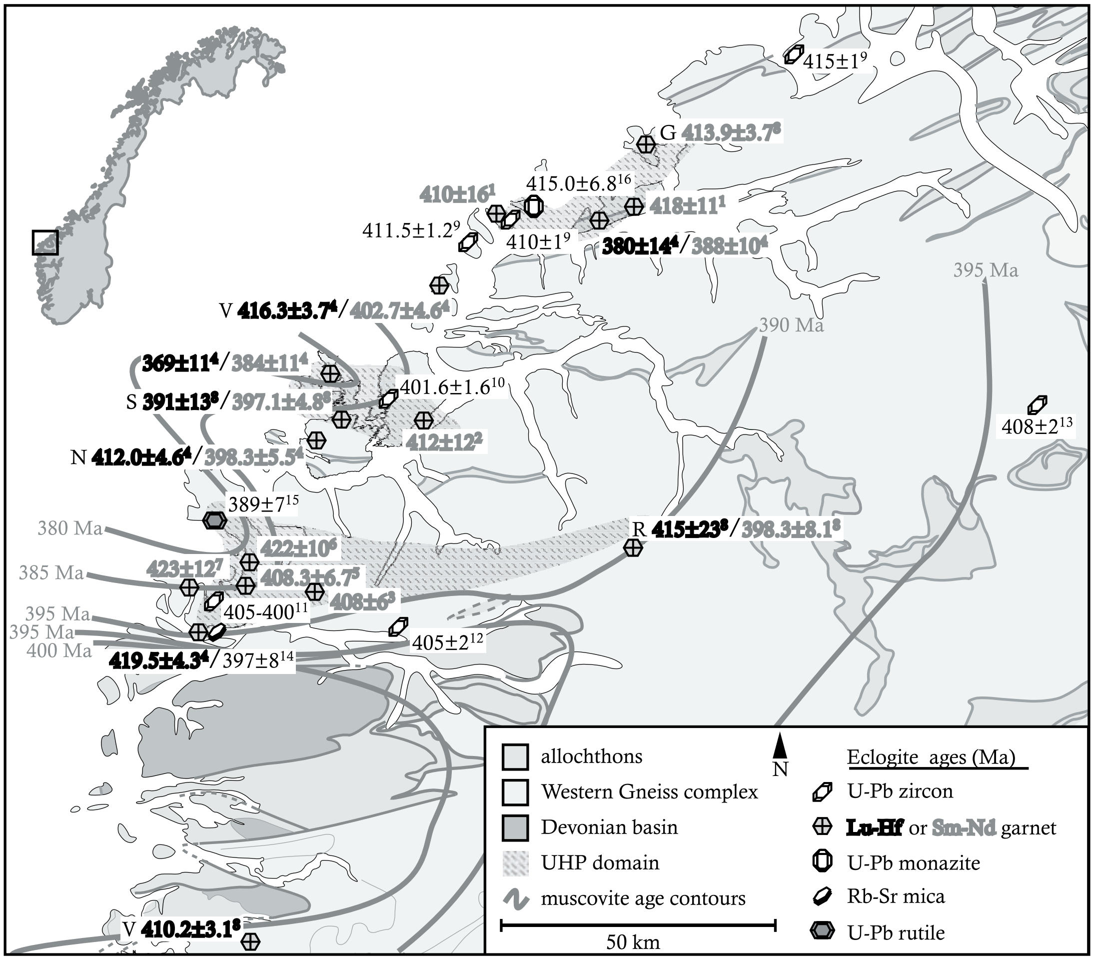

Figure 1. Western Gneiss Region, western Norway, showing the following eclogite ages, Sm-Nd and Lu-Hf: Values with superscript numbers are from 1, *Mørk and Mearns* [1986]; 2, *Jamtveit et al.* [1991]; 3, *Mearns* [1986]; 4, *Kylander-Clark et al.* [2007] (V, Vigra; N, NW Gurskøy); 5, *Carswell et al.* [2003a]; 6, H. K. Brueckner (personal communication, 2007); 7, *Griffin and Brueckner* [1980]; 8, this study (G, Gossa; R, Geiranger; V, Vollstein). U-Pb zircon, 9, *Krogh et al.* [2004]; 10, *Carswell et al.* [2003b]; 11, *Root et al.* [2004]; 12, *Young et al.* [2007b]; 13, *Kylander-Clark et al.* [2007]. Rb-Sr, 14, *Griffin and Brueckner* [1985]. U-Pb rut-omph, 15, *Schärer and Labrousse* [2003]. U-Pb monazite, 16, *Terry et al.* [2000a]. The ^{40}Ar/^{39}Ar K-white mica age contours, *Hacker et al.* [2006].

as high as 800°C and 3.4 GPa (Figure 2) [e.g., *Griffin et al.*, 1985; *Andersen et al.*, 1991; *Cuthbert et al.*, 2000]. UHP eclogites are found along the Atlantic coast in three distinct domains (Figure 1) [*Root et al.*, 2005], the northernmost of which contains the highest peak pressures and temperatures [*Dobrzhinetskaya et al.*, 1995; *van Roermund and Drury*, 1998; *Terry et al.*, 2000b; *van Roermund et al.*, 2001; *Carswell et al.*, 2006]. Metamorphic grade and peak pressures decrease eastward across the Western Gneiss Region toward the foreland, such that the easternmost reported eclogite is more than 150 km east of the coast. This metamorphic gradient is interpreted to reflect down-to-the-west subduction. The peak UHP metamorphism was followed by a pervasive amphibolite facies overprint from pressures of ~1.5 GPa down to 0.5 GPa (~45 to 15 km) during near-isothermal exhumation to midcrustal depths (summary by *Hacker* [2006]).

[7] Attempts to determine the age of the UHP metamorphism began with *Griffin and Brueckner*'s [1980] pioneering Sm-Nd work on eclogites (Figure 3). They reported a broad range of ages, 447–407 Ma, from which they selected an average age of 425 Ma. Subsequent Sm-Nd work (*Mearns* [1986] (recalculated by R. B. Root), *Mørk and Mearns* [1986], and *Carswell et al.* [2003a]) produced only younger ages, 412–408 Ma. More recent work on the U-Pb system in zircon gave ages of 415–400 Ma [e.g., *Carswell et al.*, 2003b; *Krogh et al.*, 2004; *Root et al.*, 2004; *Young et al.*, 2007a], and *Root et al.* [2004] drew on these data to conclude that the older Sm-Nd ages were mixed ages that were contaminated by older cores that predate the UHP event. Our Sm-Nd ages, as well as the first Lu-Hf ages from

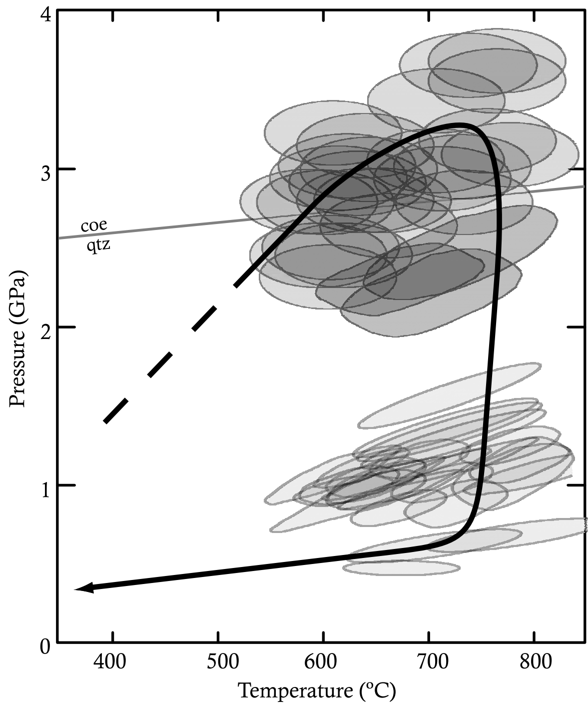

Figure 2. *P-T* history of the Western Gneiss Region after *Hacker* [2006], showing peak conditions of ~750°C and 3.4 GPa, followed by near-isothermal decompression to midcrustal levels; coe, coesite; qtz, quartz.

Norway, span a large range of 419.5 ± 4.3 to 369 ± 11 Ma [*Kylander-Clark et al.*, 2007], and these have been interpreted to confirm a broad age range for eclogite facies metamorphism. The age of the amphibolite facies overprint is constrained by ~395–390 Ma titanite, zircon and monazite ages [*Tucker et al.*, 1990; *Terry et al.*, 2000a; *Krogh et al.*, 2004; *Tucker et al.*, 2004; *Kylander-Clark et al.*, 2008], and $^{40}Ar/^{39}Ar$ muscovite ages of 400 Ma to 374 Ma (summary by *Hacker* [2006]). These data require exhumation from UHP depths of 120 km to midcrustal depth of 15 km in ~5–15 Ma.

3. New Lu-Hf and Sm-Nd Ages

[8] The Lu-Hf and Sm-Nd ages we previously reported [*Kylander-Clark et al.*, 2007] were obtained from a relatively restricted portion of the WGR within and around the UHP domains. Here we report ages from four eclogite localities that were selected to broaden the areal coverage to test the proposal that protracted UHP metamorphism occurred over a broad region. The combination of Lu-Hf and Sm-Nd ages from the same sample separates is advantageous, as it yields a minimum duration of garnet stability for any given sample, and thus provides a direct constraint on the duration of metamorphism. Because the distribution coefficient for Lu in garnet is relatively high with respect to other major eclogite phases, such as omphacite [*McKenzie and O'Nions*, 1991], and there are no minor phases that control the budget of Lu, the bulk of the Lu is sequestered in the core during garnet growth. Thus, unless the temperature exceeded the blocking temperature for the Lu-Hf system, Lu-Hf ages are biased toward early garnet growth, and this generalization holds true over a wide range of garnet growth mechanisms [*Skora et al.*, 2006]. The distribution coefficient of Sm in garnet, on the other hand, is much less than that of Lu. Thus, unless the temperature exceeded the blocking temperature for the Sm-Nd system, Sm-Nd ages tend to represent the average or later stages of garnet growth. Therefore, the difference between the Lu-Hf and Sm-Nd ages for samples can be used as a minimum estimate for the duration of garnet growth, i.e., the duration of HP and UHP conditions, provided that the samples never significantly exceeded the blocking temperature for either system. This appears to be the case in the WGR: The Sm-Nd garnet ages of eclogites are equivalent to U-Pb zircon ages that are interpreted to represent the eclogite facies metamorphism of nearby sample localities (see section 3.3).

[9] Sample preparation and analysis followed that outlined by *Kylander-Clark et al.* [2007] and *Lapen et al.* [2003, 2004]. Analyses were performed on a Micromass IsoProbe ICP-MS (Lu-Hf) and VG Sector 54 TIMS (Sm-Nd) at the University of Wisconsin, Madison. Pressure and temperature estimates were obtained from minerals analyzed on the Cameca SX-50 microprobe at the University of

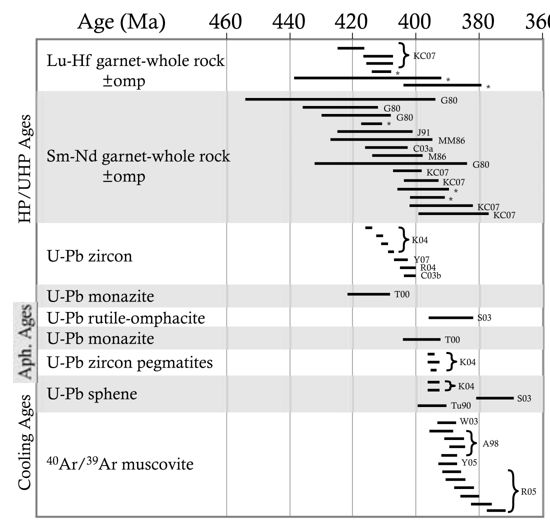

Figure 3. Geochronology from the Western Gneiss Region, showing ages of prograde through peak conditions, postpeak amphibolite facies metamorphism, and cooling; omp, omphacite; Aph, amphibolite. KC07, *Kylander-Clark et al.* [2007]; MM86, *Mørk and Mearns* [1986]; J91, *Jamtveit et al.* [1991]; M86, *Mearns* [1986]; C03a, *Carswell et al.* [2003a]; G80, *Griffin and Brueckner* [1980]; K04, *Krogh et al.* [2004]; C03b, *Carswell et al.* [2003b]; R04, *Root et al.* [2004], Y07, *Young et al.* [2007b]; S03, *Schärer and Labrousse* [2003]; Tu90, *Tucker et al.* [1990]; T00, *Terry et al.* [2000a]; W03, *Walsh* [2003]; A98, *Andersen et al.* [1998]; Y05, *Young* [2005]; R05, *Root et al.* [2005]; asterisk, this study.

Table 1a. Lutetium-Halfnium Isotope Data for Eclogites From the Western Gneiss Region, Norway[a]

Sample[b]	Concentration (ppm) Lu	Hf	$^{176}Lu/^{177}Hf$	$^{176}Hf/^{177}Hf$	Age (Ma)	$\varepsilon_{Hf(0)}$[c]
K5622A2 (Vollstein)						
grt (107.8)	0.23	0.10	0.3255	0.285356 ± 13		
cpx (29.6)	0.00	0.24	0.0010	0.282868 ± 19		
wr (91.8)	0.14	0.42	0.0485	0.283223 ± 10	410.2 ± 3.1	12
P5701A (Sandvik)						
grt[d] (95.4)	0.42	0.83	0.0719	0.282914 ± 4		
grt[e] (86.8)	0.42	1.05	0.0568	0.282819 ± 5		
cpx (53.3)	0.01	1.01	0.0009	0.282396 ± 5		
wr (44.7)	0.20	1.66	0.0173	0.282527 ± 4	391 ± 13	−4.7
E1612Q5 (Geiranger)						
grt[3] (70.7)	0.53	1.23	0.0617	0.282828 ± 5		
grt[4] (93.4)	0.54	1.36	0.0565	0.282817 ± 3		
cpx (37.0)	0.00	0.52	0.0013	0.282369 ± 7		
wr (183.4)	0.30	2.25	0.0192	0.282518 ± 3	415 ± 23	−5.3

[a]Analysis accomplished by isotope dilution multicollector plasma mass spectrometry at University of Wisconsin, Madison. Decay constant used for ^{176}Lu is 1.865×10^{-11} a^{-1} [*Scherer et al.*, 2001]. Errors in Hf isotope ratios are expressed as 2SE from internal measurements and refer to least significant digits. Isochron ages were calculated using Isoplot v. 3.0. Errors calculated for ages are based solely on external reproducibility of spiked standards and whole rock samples (errors for individual analyses are negligible): $^{176}Lu/^{177}Hf = 0.2\%$, $^{176}Hf/^{177}Hf = 0.005\%$. Minerals are grt, garnet; cpx, clinopyroxene; wr, whole rock.

[b]Sample weights are listed in mg.

[c]The $\varepsilon_{Hf(0)}$ was calculated using present-day ratios of $^{176}Hf/^{177}Hf = 0.282772$ and $^{176}Lu/^{177}Hf = 0.0334$ for CHUR [*Blichert-Toft and Albarède*, 1997].

[d]Purer garnet separate.

[e]Less pure garnet separate.

California, Santa Barbara. All quoted age uncertainties are 2σ and exclude uncertainty in decay constants.

3.1. Sample Descriptions

[10] Sample P5701A from Sandvik, northern Gurskøy (Figure 1) is an eclogite that contains little evidence for retrogression. The sample consists of agglomerations of hypidioblastic to xenoblastic garnet 0.1–1 mm in diameter (~55 vol %). Clinopyroxene (40 vol %) up to 0.5 cm wide and 2 cm long defines a millimeter-scale foliation and has minor amphibole replacement. Biotite (<5 vol %) is ~1 mm long and aligned parallel to the foliation. Minor opaque minerals occur along grain boundaries. The nearest eclogite facies pressure and temperature estimates are 795°C and 3.2 GPa from Hareidlandet, ~10 km to the NE [*Carswell et al.*, 2003b].

[11] Sample E1612Q5 is an eclogite from Hellesylt (Figure 1) [*Walsh et al.*, 2007]. It contains millimeter-scale layers of hypidioblastic garnet 0.1–1 mm in diameter and ~2-mm-long omphacite. Rutile (<2 vol %) occurs as isolated ~0.2-mm grains. Pressures of 2.8 GPa and temperatures >700°C have been estimated from samples within a few kilometers [*Walsh and Hacker*, 2004].

[12] Sample NOR205 is an unretrogressed eclogite from the Blåhø Nappe on Gossa (Figure 1), described by *Hollocher et al.* [2007]. Garnet (~30 vol %) is 2–4 mm and poikiloblastic, containing clinopyroxene, calcite, and amphibole. Clinopyroxene (~20 vol %) is 1–5 mm and exhibits strong undulatory extinction and subgrains. Orthopyroxene (~20 vol %) is ~2–5 mm and has few subgrains. Amphibole (~20 vol %) is 0.2 mm and hypidioblastic. Minor phases include rutile and opaque minerals (<2 vol %). Pressure-temperature estimates from nearby UHP rocks are ~800°C and ~3.3 GPa [*Carswell et al.*, 2006].

[13] Sample K5622A1 is an unfoliated and unretrogressed eclogite from Vollstein (Figure 1) composed of equal portions of clinopyroxene (~0.2–1 mm) and garnet. Garnet is idioblastic, ~0.5 mm, and has darker pink cores with inclusions of amphibole and epidote. Amphibole (~10 vol %) is xenoblastic and ~0.2–1 mm in diameter. Minor phases include phengite, rutile, and epidote. Thermobarometry using garnet-clinopyroxene-phengite equilibria [*Krogh Ravn and Terry*, 2004] produced temperatures and pressures of 615°C and 2.4 GPa.

3.2. Lu-Hf and Sm-Nd Ages

[14] Our new Lu-Hf and Sm-Nd data are presented in Table 1a and 1b and Figure 4. All the samples yielded relatively low MSWD values (≤2.5) for all fractions analyzed. One sample generated a high-precision three-point Lu-Hf isochron, and three samples generated relatively high-precision four-point Sm-Nd isochrons. Two samples for which we obtained both Lu-Hf and Sm-Nd ages (E1612Q5 and P5701A) yielded relatively low parent/daughter ratios for the garnet fractions, and thus low-precision ages. This is likely the result of a relatively low Lu/Hf ratio in the whole rock and/or a larger modal proportion of garnet, rather than the presence of high-Hf inclusions in the garnet fractions. Given the high distribution coefficient for Lu in garnet, the bulk of the Lu is likely sequestered in garnet cores, whereas the Hf concentration should be relatively constant from core to rim [*Lapen et al.*, 2003; *Skora et al.*, 2006]. Thus, the larger the modal proportion of garnet, or the smaller the Lu/Hf ratio in the whole rock, the smaller the Lu/Hf ratio in the bulk garnet

Table 1b. Samarium-Neodymium Isotope Data for Eclogites From the Western Gneiss Region, Norway[a]

Sample[b]	Concentration (ppm) Sm	Nd	$^{147}Sm/^{144}Nd$	$^{143}Nd/^{144}Nd$	Age (Ma)	$\varepsilon_{Nd(0)}$[c]
P5701A (Sandvik)						
grt (86.8)	0.93	0.47	1.205	0.515043 ± 12		
cpx (53.3)	3.27	10.91	0.182	0.512365 ± 13		
wr (44.7)	1.75	5.92	0.179	0.512383 ± 9	397.1 ± 4.8	−4.3
E1612Q5 (Geiranger)						
grt[d] (70.7)	1.31	0.95	0.837	0.514085 ± 9		
grt[e] (93.4)	1.31	1.01	0.792	0.513986 ± 8		
cpx (37.0)	1.91	5.68	0.204	0.512467 ± 10		
wr (183.4)	1.98	5.55	0.216	0.512452 ± 12	398.3 ± 8.1	−4.1
NOR205 (Gossa)						
grt[3] (37.3)	1.26	0.59	1.301	0.515909 ± 11		
grt[4] (33.6)	1.17	0.57	1.250	0.515789 ± 14		
cpx (35.9)	0.78	2.47	0.191	0.512906 ± 14		
wr (223.7)	1.59	3.80	0.254	0.513083 ± 7	413.9 ± 3.7	5.6

[a]Analysis accomplished by isotope dilution multicollector plasma mass spectrometry at University of Wisconsin, Madison. Decay constant used for ^{147}Sm is 6.54×10^{-12} a^{-1}. Errors in Nd isotope ratios are expressed as 2SE and refer to least significant digits. Isochron ages were calculated using Isoplot v. 3.0. Errors calculated for ages are based solely on external reproducibility of spiked standards and whole rock samples (errors for individual analyses are negligible): $^{147}Sm/^{144}Nd$ = 0.5%, $^{143}Nd/^{144}Nd$ = 0.005%.

[b]Sample weights are listed in mg.

[c]The $\varepsilon_{Nd(0)}$ was calculated using present-day ratios of $^{146}Nd/^{144}Nd$ = 0.7219 and $^{143}Nd/^{144}Nd$ = 0.512638 for CHUR.

[d]Purer garnet separate.

[e]Less pure garnet separate.

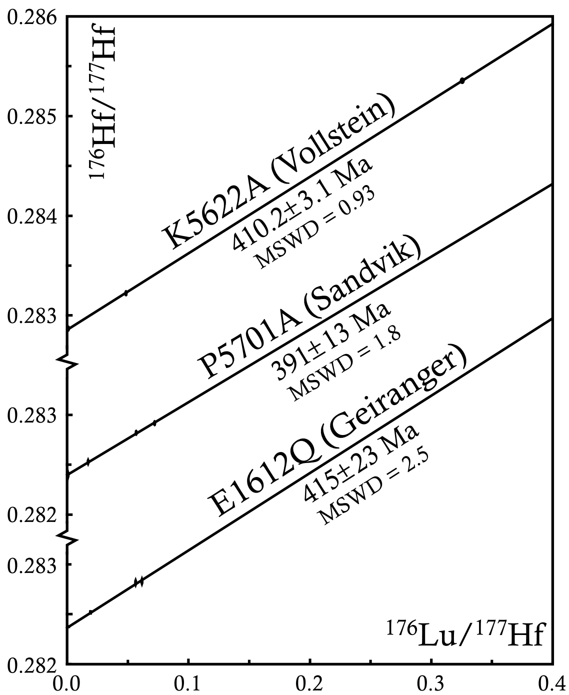

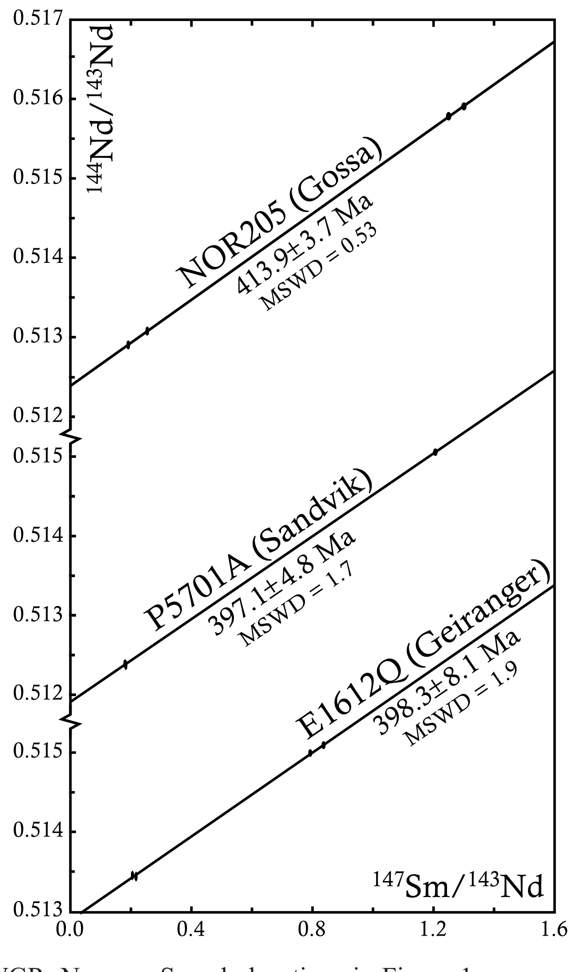

Figure 4. New Sm-Nd and Lu-Hf ages from the WGR, Norway. Sample locations in Figure 1.

separate. Our previous Lu-Hf data set for WGR eclogites produced this same phenomenon [*Kylander-Clark et al.*, 2007]. Nevertheless, any significant volume of high-Hf inclusions could not have significantly affected the age yielded by both samples. If high-Hf inclusions, such as zircon, were significantly older than the enclosing garnet, the inclusion-rich garnet fraction would have lower $^{176}Hf/^{177}Hf$ ratios relative to the inclusion-poor garnet fraction [*Prince et al.*, 2000]; this is not the case in either of our samples. Furthermore, variable amounts of old zircon in each of the handpicked separates would yield data that are not isochronous.

[15] The garnet ages span more than 20 Ma, from 415 Ma to 391 Ma. Because of the large uncertainty for the youngest age, a more realistic span of ~17 ± 6 Ma is given by the difference between two high-precision ages of 413.9 ± 3.7 Ma and 397.1 ± 4.8 Ma, where the uncertainty in the span in ages is estimated using the square root of the sum of the squares of the errors of the two ages. The Sm-Nd age from Gossa (NOR205), 413.9 ± 3.7 Ma, is the northernmost four-point isochron obtained from the WGR; it is equivalent to Sm-Nd garnet, U-Pb zircon and U-Pb monazite ages from nearby localities (Figure 1) [*Griffin and Brueckner*, 1980; *Terry et al.*, 2000a; *Krogh et al.*, 2004]. The Sm-Nd age of 398.3 ± 8.1 Ma obtained from Hellesylt (E1612Q5) is equivalent to the 396 ± 10 Ma U-Pb zircon SIMS age obtained by *Walsh et al.* [2007] for the same sample. The Lu-Hf age from E1612Q5 overlaps its Sm-Nd age, but errors are high because there is little spread in Lu/Hf ratios. Sample P5701A from north Gurskøy yielded a high-precision Sm-Nd age of 397.1 ± 4.8 Ma, similar to the Sm-Nd age of 398.3 ± 5.5 Ma from west Gurskøy [*Kylander-Clark et al.*, 2007]. The Lu-Hf age of 391 ± 13 Ma for this sample lies within error of its Sm-Nd age, although the errors for the Lu-Hf age are relatively high because of the limited spread in Lu/Hf ratios. The Lu-Hf age of 410.2 ± 3.1 from sample K5622A overlaps Lu-Hf ages from the central WGR [*Kylander-Clark et al.*, 2007] and is the first eclogite age obtained from the southern WGR (Figure 1).

3.3. Discussion of the Geochronology Data Set

[16] Our new ages, combined with the existing geochronologic data set for the WGR, strongly suggest that the (U)HP metamorphism of the WGR occurred over a 20 Ma period: U-Pb zircon and monazite ages for eclogites at (U)HP conditions range from 415 to 400 Ma, high-precision Lu-Hf ages range from 420 to 410 Ma, and high-precision Sm-Nd ages range from 412 to 397 Ma (Figure 1). This conclusion is reinforced by the fact that this data set comes from three different isotopic systems from measurements made in different laboratories.

[17] These eclogite ages come from a large portion of the WGR, spanning ~220 km north to south within the UHP hinterland and 60 km from the hinterland in the west toward the foreland in the east. Does such a long span of ages mean that this entire area was subjected to (U)HP metamorphism for 20 Ma as a large block, or is it possible that this large region comprises different slices that had distinct *P-T* histories and hence underwent (U)HP metamorphism at different times? There are two observations that argue in favor of the former and against the latter.

[18] 1. There are no UHP domains that have yielded a narrow range of eclogite ages. For example, the Nordfjord UHP domain yields a Lu-Hf age at Verpeneset ~20 Ma older than the U-Pb zircon age of Flatraket, only 8 km distant. The Nordøyane UHP domain has produced U-Pb and Sm-Nd ages of 415–410 Ma, but also a Sm-Nd age of 388 ± 10 Ma (Figure 1). It is possible, albeit unlikely, that the young age does not represent eclogite facies conditions [*Kylander-Clark et al.*, 2007] and thus could indicate that the northern WGR underwent a different prograde history than the WGR south of the Nordøyane UHP domain. An amphibolite facies shear zone that cuts through the southern portion of this region [*Terry and Robinson*, 2003, 2004] would support this hypothesis, but it separates the ~412 Ma Løvsøya eclogite from similar age eclogites to the north [*Terry et al.*, 2000a; *Krogh et al.*, 2004]. No other significant structures have been recognized.

[19] 2. Two eclogite localities, Vigra and NW Gurskøy (Figure 1), have Lu-Hf ages that are 14 Ma older than their respective Sm-Nd ages, indicating that garnet growth spanned at least that long [*Kylander-Clark et al.*, 2007]. Thus, the ~20 Ma spread in ages throughout the WGR is best explained by long-term residence of a ~220 km × ~60 km piece of subducted continental crust at high-pressure conditions.

[20] Although the (U)HP eclogite facies metamorphism was preceded and followed by metamorphic episodes in which garnet was stable, it is unlikely that the garnet ages reflect mixtures of garnet of a variety of ages. First, the dated samples do not contain significant retrograde mineral assemblages. Second, although a Barrovian amphibolite facies metamorphism at ~700°C and 1.0–1.5 GPa occurred between 445 and 432 Ma over much of the allochthons in the foreland [*Hacker and Gans*, 2005], this event has not been recognized in the crystalline WGC. Third, although Precambrian (~950–900 Ma) granulite facies metamorphism is recognized in a small portion of the crystalline rocks of the WGR [*Cohen et al.*, 1988; *Røhr et al.*, 2004; *Root et al.*, 2005; *Glodny et al.*, 2008], and in some places is overprinted by eclogite facies metamorphism [*Wain et al.*, 2001], these two events produced distinctly different major element zoning in garnets. The samples studied here contain no evidence of granulite facies garnet compositions. In addition, because the granulite facies metamorphism predated the eclogite facies metamorphism by 500 Ma, a sample that contains a mixed population of garnets should not produce a multipoint, low-MSWD isochron typical of our data. Furthermore, Caledonian garnets that contain an inherited component of ~950 Ma garnet could be no more than 5% inherited to yield an age between 425 and 400 Ma. All of the 16 sample locations listed in Figure 1 that report either a Lu-Hf age, Sm-Nd age, or both, yield ages between 425 and 400 Ma. Because it is no more likely for a garnet to contain 5% inheritance than, for example, 50% inheritance, the span in ages likely represents the minimum duration of HP conditions during the Caledonian event.

[21] Some eclogites in the WGR had a prograde history that passed through amphibolite or blueschist facies conditions, during which time garnet growth likely occurred [*Krogh*, 1980, 1982] at pressures of ~1 GPa and higher. Because the pressures of eclogite facies metamorphism in the WGR ranged up to 3.4 GPa [*Terry et al.*, 2000a; *Krogh Ravn and Terry*, 2004; *Carswell et al.*, 2006], garnet growth probably occurred at depths of ~33 km to 112 km (assuming 3 g cm^{-3}). The inferred ~20 Ma interval of garnet growth, therefore, is interpreted to reflect prograde growth during burial at an average rate of <4 mm a^{-1}.

4. Thermal Model of Long-Duration (U)HPM Tectonism

[22] Although it is generally assumed that UHP terranes spent only a few million years at UHP conditions, at least four regions appear to have spent 15–20 Ma at such conditions: the Norwegian UHP terrane (this paper), the Dabie-Sulu terrane of eastern China [*Hacker et al.*, 2006], the North Qaidam terrane of western China [*Mattinson et al.*, 2006], and the northeast Greenland eclogite province [*McClelland et al.*, 2006]. Long-term metamorphism at UHP conditions is a puzzle for one simple reason: the characteristic thermal diffusion distance for 15–20 Ma is 20–25 km (assuming a thermal diffusivity of 10^{-6} m s^{-2} [*Turcotte and Schubert*, 2002]), suggesting that if UHP terranes are only a few kilometers thick, they cannot survive such a lengthy immersion in the hot mantle without melting [*Root et al.*, 2005]. In this section we use a simple thermal model to explore the parameter space (i.e., subduction rate and initial thermal profile) that might permit terranes (1) to survive 15–20 Ma at HP conditions without exceeding the maximum temperatures observed in the WGR and (2) to undergo near-isothermal return to midcrustal levels.

4.1. Model Parameters

[23] The thermal model is a 395 × 195 km (5-km node spacing) 2-D transient heat flow model that uses the alternating direction, implicit, finite difference method described by *Hacker* [1990]. The upper plate is continental and the lower plate is continental or oceanic (see below). The continental crust is 40 km thick and has a radiogenic heat production rate of 1.68, 1.04, and 0.21 μW m^{-3} in the upper (top 12 km), middle (12–23 km), and lower (23–40 km) crust, respectively (average for continental crust [*Rudnick and Gao*, 2003]). The upper boundary of the model is held at 0°C, the basal boundary condition is a constant heat flow of 25 μW m^{-2}, and the lateral boundary conditions are a downward increasing constant temperature gradient. The angle of subduction of the lower plate is 45°. Convection in the mantle wedge is prescribed in a simplified form; corner flow occurs at a constant flow rate everywhere the temperature exceeds 1000°C (Figure 5a). The time step was 0.01 Ma for subduction and 0.005 Ma for exhumation.

[24] The two primary controls on the thermal structure of a subducting plate are subduction velocity and initial thermal structure [e.g., *van Keken et al.*, 2002]. We model two end-member scenarios: (1) subduction of a continental lower plate into a thermal steady state, Andean-style subduction zone and (2) intracontinental subduction. In both scenarios we vary the continental subduction rate and initial thermal gradient to explore the effects on the thermal evolution of the system. In scenario 1 we use an upper plate thermal gradient of 15°C km^{-1}, similar to the thermal structure of Andean-style subduction zones [*van Keken et al.*, 2002]. For simplicity, the subducting oceanic plate is given the thermal structure of the subducting continental plate. The oceanic subduction velocity is 47 mm a^{-1}, equivalent to the average subduction rate of Andean-style subduction zones [*Jarrard*, 2003; *Lallemand et al.*, 2005] and the model is run for 30 Ma to reach steady state thermal conditions. The model is then run with the prescribed continental subduction velocity until the continental material reaches a depth of ~105 km (~3.2 GPa) or 150 km (~5 GPa).

[25] The initial thermal gradients for the continental material were varied from 10°C km^{-1} to 25°C km^{-1}. The vertical component of the subduction velocity was varied between 1 and 21 mm a^{-1}, a range that encompasses all modern convergence zones with continental lower plates. Maintenance of all points in the subducted continent within the garnet-stable depth range requires subduction rates of<4 mm a^{-1} for metamorphic durations of 20 Ma.

[26] After subduction, the motion of the upper 40 km of the lower plate was reversed to simulate 85 km of exhumation from a maximum depth of 105 km to a midcrustal depth of 20 km (Figure 5b). The vertical exhumation rate was 33 mm a^{-1}, corresponding to 85 km of exhumation in 5 Ma, as suggested by geochronology (see section 3.3).

4.2. Model Results

[27] Examples of the calculated temperature field are shown in Figure 6a. As expected, temperatures in the core of the subducted slab are relatively low if the initial slab thermal gradient is low (Figure 6a, left) or the subduction rate is high (Figure 6a, right). Only for vertical subduction rates of ~1–11 mm a^{-1} (~2–16 mm a^{-1} subduction at 45°) and slab thermal gradients of 10–25°C km^{-1} do the temperatures at 105 km depth match the 700–800°C temperatures observed in Norway. During exhumation, temperatures at the top of the lower plate always decrease, generally by more than 200°C. Temperatures at depth in the slab increase for fast subduction ($\geq$ 16 mm a^{-1}), and decrease for slow subduction ($\leq$11 mm a^{-1}).

[28] Figure 6b shows examples of the temperature field in the crust after exhumation. Only for vertical subduction rates of <10 mm a^{-1} (<15 mm a^{-1} subduction at 45°) do the models produce the near-isothermal exhumation to midcrustal depths observed in Norway. Figure 6c shows T_d, the sum of the temperature deviations at each node from 750°C at peak pressure and after exhumation, calculated as

$$T_d = |750°C - T_{at\_peak\_pressure}| + |750°C - T_{at\_15\_km}|$$

The white domains of Figure 6c indicate conditions that produce near-isothermal paths; cooler colors show UHP

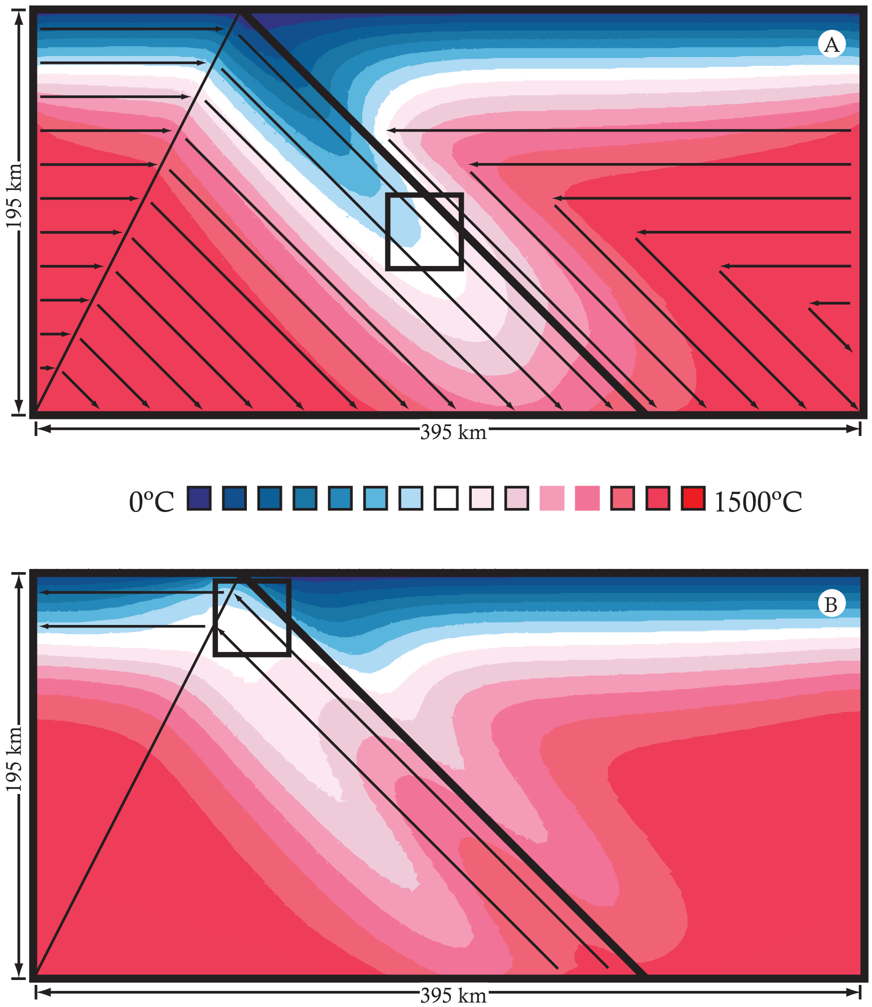

Figure 5. Flow lines for thermal model showing crustal sections represented in Figure 6 and used to make calculations shown in Figure 7 (black squares). (a) Subduction. (b) Exhumation. Convection in the mantle wedge is dependent on initial thermal gradient and is defined in this model at ~1000°C. The temperatures shown in this example result from intracontinental subduction with an initial thermal gradient of 25°C km^{-1} and a subduction velocity of 11 mm a^{-1}.

metamorphism that is colder than 750°C, or cooling during exhumation, whereas warmer colors show UHP metamorphism hotter than 750°C (slow subduction), or warming during exhumation (fast subduction). The cooler colors at the top and upper left of each diagram reflect excessive cooling, as the crust has reached shallow levels and been cooled from above.

[29] Figure 7 summarizes the average temperature and temperature deviation, T_d, for crust that reaches 105 to 90 km depth. Only the middle 28 km of the crust is shown; the outer portion of the crust becomes too hot during subduction and/or too cold during exhumation to be representative of the exposed terrane in Norway, as discussed in section 4.3.1. For 105 km of subduction, only intracontinental subduction is shown because the Andean subduction scenario only yields temperatures higher than 700°C if subduction rates are unrealistically slow (~1 mm a^{-1} or less). From these considerations, we infer that vertical subduction rates must be slow (≤4 mm a^{-1}; equivalent to ≤6 mm a^{-1} subduction velocity) to maintain the subducted continent in the garnet stability field (30 to 60–105 km depth) for 20 Ma, as well as produce 750°C UHP eclogites during subduction and near-isothermal exhumation. The main difference between the Andean and the intracontinental subduction scenarios is that continental subduction in the Andean setting yields cooler temperatures than intracontinental subduction, for any given set of initial conditions.

[30] The largest portions of crust undergo near-isothermal decompression at ~750°C (lowest T_d values) for subduction to either 105 or 150 km depth if the slab is initially hot (pale colors in Figure 7c). The Andean subduction scenario achieves minimum T_d values for 150 km of subduction

and exhumation at subduction rates of <2 mm a^{-1}; this rate and depth require >75 Ma of subduction, which is incompatible with the Norway geochronology data set. The intracontinental subduction scenario yields the lowest T_d values at subduction rates of ~6 and 11 mm a^{-1} for 150 and 105 km of subduction, respectively. For vertical subduction rates of 2–4 mm a^{-1}, the same scenario yields minimum T_d values for moderate initial thermal gradients (15–20°C km^{-1}) for subduction to 105 km and higher initial thermal gradients (20–25°C km^{-1}) for subduction to 150 km. Intracontinental subduction also leads to larger variation in average temperature and T_d values, reflecting the greater variation in the initial upper plate temperature profiles. These scenarios are compatible with the Norway geochronology database.

4.3. Discussion of the Modeling

4.3.1. Implications

[31] Because rocks over a large region of the WGR followed similar *T-t* paths (Figure 2) and recorded peak pressures mostly ≤3.2 GPa, model runs that yield the lowest T_d values produce *P-T-t* paths that are closest to those observed in Norway. Coupled with the constraints that (1) vertical subduction rates of 2–4 mm a^{-1} are required by the ~20-Ma duration of WGR UHP metamorphism and (2) decompression was rapid and nearly isothermal, our modeling results favor an intracontinental setting in which the slab had a moderate to hot geothermal gradient (15–25°C km^{-1}) and was subducted at a vertical rate of ~2–4 mm a^{-1}. The models do not preclude cooler thermal gradients or Andean-style subduction, but on the basis of the model results, these possibilities seem less likely.

[32] The simulations also make some useful predictions.

[33] 1. Rocks that were farther up dip of the UHP domain during subduction, should have reached lower temperatures and decompressed isothermally. In Norway, eclogites that record lower temperatures and pressures are east of the UHP domains [*Cuthbert et al.*, 2000; *Young et al.*, 2007a] and are overprinted by amphibolite facies assemblages that formed at temperatures similar to the eclogite facies temperatures [*Walsh and Hacker*, 2004].

[34] 2. Rocks that were farther down dip of the UHP domain should have reached higher temperatures. Such rocks are yet unrecognized in the WGR and may not be exposed because of rifting of the Atlantic Ocean.

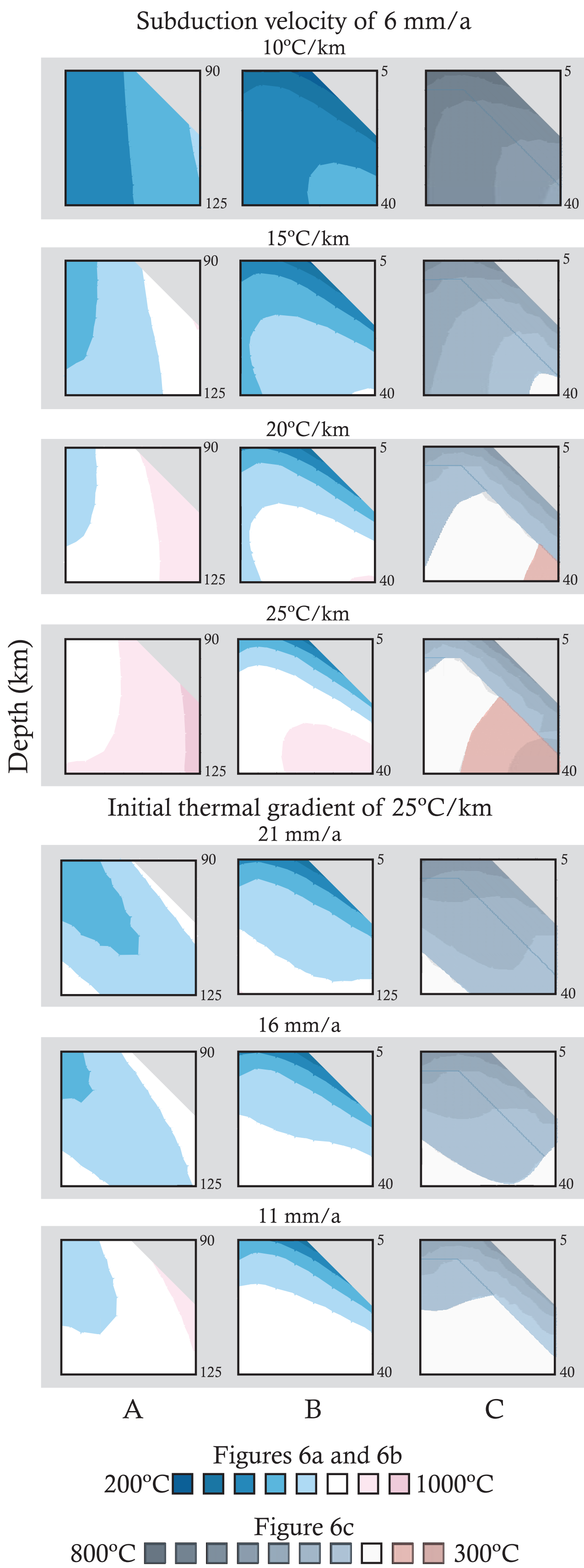

Figure 6. (a) Temperatures of the crust, in a 35 × 35 km section (black square from Figure 5a) from 90 to 105 km following 150 km of intracontinental subduction, using varied initial thermal gradients and subduction rates. (b) Exhumation of each crustal section in Figure 6a, after 85 km of exhumation. (c) Deviation from isothermal decompression at 750°C following exhumation. Warm colors show excessive temperatures upon subduction or exhumation; cooler colors show cold initial temperatures or excessive cooling. The upper plate (top right) is shaded out in each diagram for simplicity.

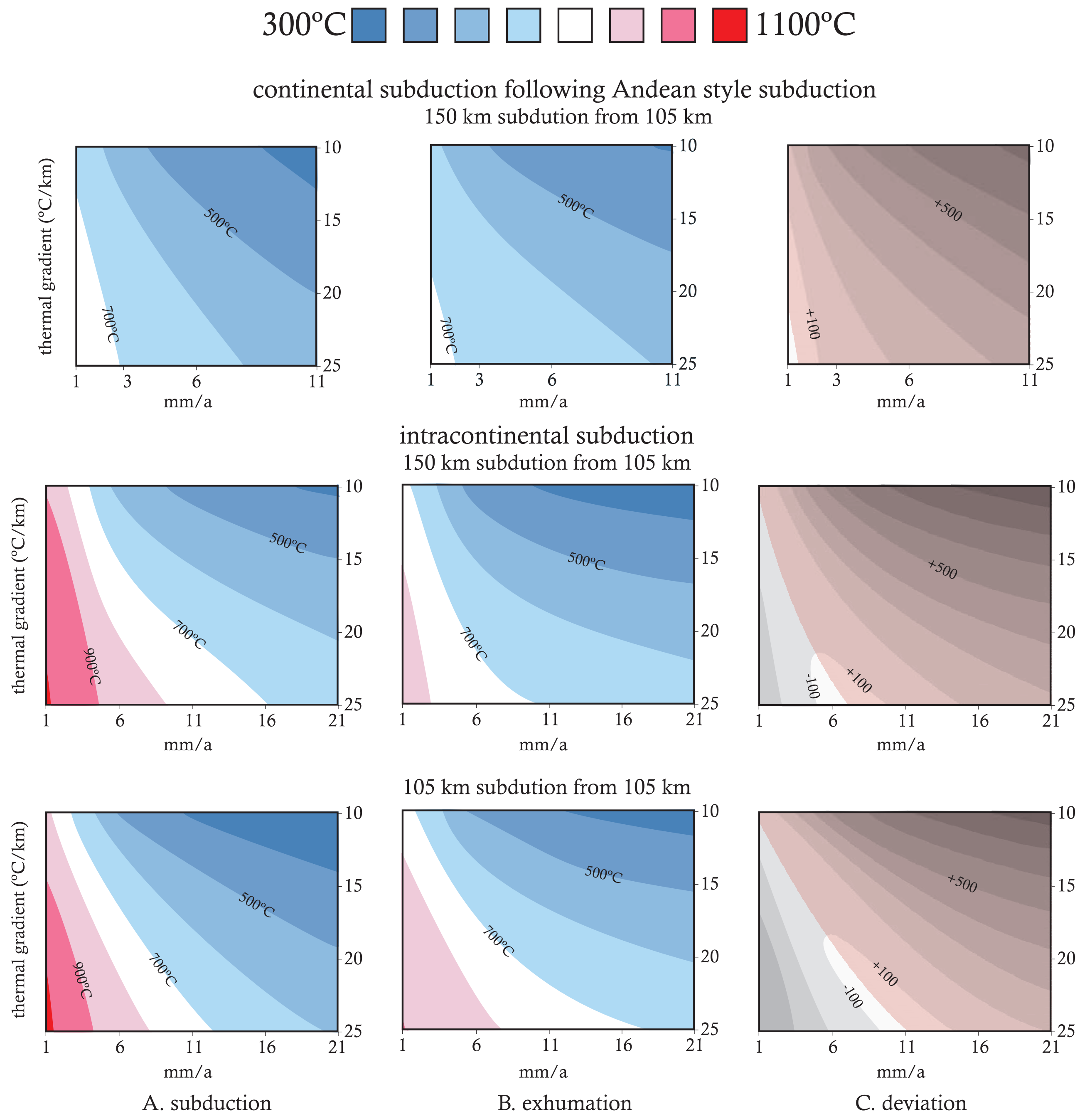

Figure 7. (a) Average temperatures for the middle ~28 km of the crust, from 90 to 105 km following 150 or 105 km of subduction, with variable subduction velocities and initial thermal gradients of the lower plate. (b) The portion of crust in Figure 7a, after 85 km of exhumation. (c) Deviation from isothermal decompression at 750°C of the crustal section represented in Figures 7a and 7b.

[35] 3. The downdip thermal gradient in satisfactory scenarios ranges from ~3 to 5°C km^{-1}, similar to that observed in Norway [e.g., *Young et al.*, 2007a].

4.3.2. Limitations

[36] There are several simplifications in our model that may produce uncertainties relative to the thermal-mechanical conditions that are expected during UHP metamorphism. These uncertainties are discussed in detail below; however, our model yields similar *P-T* paths of more complicated thermal-mechanical models [*Warren et al.*, 2008], given similar initial conditions.

[37] A constant subduction velocity was assumed, and a single upper plate thermal gradient, similar to that produced by recent thermal models [e.g., *van Keken et al.*, 2002], was used to establish the thermal profile of the Andean-style margin prior to continental subduction. The thermal profile of the upper plate is essentially independent of subduction velocity and the age of the lower plate. The thermal profile of the upper plate does, however, depend on parameters, such as crustal thickness, that are not well known for Norway. Therefore, the initial thermal profile of the upper plate could have been significantly different from our model. For example, an increase of the upper plate thermal gradient by 10°C km^{-1} yields an increase of ~100°C in the lower plate at 100 km depth; such an increase in temperature allows a large portion of the crust to reach 750°C and to decompress isothermally, following reasonable vertical rates of subduction (i.e., 2–4 mm a^{-1}).

[38] Our fixed subduction angle of 45° is steeper than some active continental convergence zones (e.g., India-Asia), but shallower than others (e.g., Hindu Kush). Nevertheless, our models compare favorably to those that assumed shallower dips, such as *Roselle and Engi* [2002], who used a subduction angle of 30°. For the same vertical subduction rate and initial thermal conditions, our model produces similar temperatures at UHP depths.

[39] Frictional heating is poorly understood in subduction zones and ignored in our models. Incorporation of friction in the model would produce higher temperatures in the lower plate, with a greater effect at faster plate velocities. The heating due to friction is highest at the plate boundary and typically no greater than 100°C [e.g., *Roselle and Engi*, 2002]. Because the plate boundary cools by >200°C in our models, we anticipate that crustal cooling in excess of 100°C would still occur during exhumation if frictional heating were included. The uncertainties in frictional heating may be mitigated if we only consider the middle 28 km of the subducted crust in our discussion because it is anticipated that the middle section of crust is the most likely portion to experience isothermal decompression.

[40] We assume a simple convection model for the mantle wedge. More complex models for the upper plate have been used in other studies [e.g., *van Keken et al.*, 2002], but uncertainties in the subduction geometry during formation of the Norwegian Caledonides prevent us from exploring these. We note that our models do produce results that are similar to those obtained using more complicated models for the upper plate [e.g., *Roselle and Engi*, 2002].

[41] The subducted plate is assumed a rigid block during subduction and exhumation. The plate could thicken or thin during subduction and/or exhumation, and this deformation would affect the temperature within the slab. For example, given the same vertical subduction rate, a slab that thickened during subduction would have a colder core than a slab that did not thicken. Likewise, thinning during exhumation would allow the slab to cool more rapidly.

[42] Finally, we assume constant subduction and exhumation rates. Long-term HP conditions can be produced by temporal variation in subduction rate, such as faster subduction to near-UHP depths, followed by slower subduction at UHP depths. Likewise, a 5 Ma decompression path can occur via temporal variations in exhumation rates, such as rapid exhumation through the mantle, followed by slower exhumation through the lower crust. The more time the material in question spends at greater depths, the hotter it will be than those represented in our model.

5. Discussion of Tectonics

[43] The modeling discussed in section 4.3 suggests that HP conditions can be maintained for ~20 Ma, followed by near-isothermal decompression at 750°C, provided that (1) relatively slow subduction occurred in an intracontinental setting and (2) exhumation involved a crustal segment that was at least tens of kilometers in the minimum dimension. Subduction rates for UHP terranes as slow as a few millimeters per year were formerly thought to be unlikely because the crustal segments that went to UHP conditions were envisioned to be thin to facilitate the rapid cooling observed in UHP terranes worldwide [*Ernst and Peacock*, 1996]; during slow subduction, thin crustal sections would heat too much during subduction. In contrast, *Root et al.* [2005] explained the *P-T* history of the WGR, which remained at ~750°C from the time of UHP metamorphism to the time it reached midcrustal depths of ~15–20 km [*Terry et al.*, 2000a; *Root et al.*, 2005], through subduction of a UHP body >30 km thick. Our more detailed modeling supports this conclusion and emphasizes the observation that a more complex simulation of exhumation leads to unacceptably large cooling in at least the outer 7 km of a 40-km-thick slab (more for slower exhumation rates). We conclude that the slab must have been more than 14 km thick to allow isothermal cooling during exhumation. *Warren et al.*'s [2008] more complicated model also shows an exhumed UHP wedge that is >20 km thick. There are few geologic observations that constrain the thickness of the WGR. Seismic studies indicate that western edge of the WGR consists of a >40-km-thick section of exhumed Baltic crust, which supports our findings; however, this section may consist of imbricate slices [*Hurich*, 1996].

[44] Following near-isothermal exhumation to midcrustal depths of 20 km, the WGR cooled rapidly. Specifically, the cooling rate across the WGR varied from 15 to 50°C Ma^{-1} (~750°C–400°C in 5–15 Ma), with faster cooling in the eastern WGR. Because the characteristic thermal diffusion distance for 5–15 Ma is 12–21 km, this cooling could have been accomplished by conductive cooling from above.

[45] We conclude that UHP terranes that are large and contain evidence for a protracted period of peak or near-peak metamorphism represent one end-member of a spectrum of size–time–subduction rate parameters. We suggest that other UHP terranes that show similar traits over such large areas also may have been thick bodies from the onset of subduction through exhumation to lower to midcrustal levels. An obvious candidate is the Dabie-Sulu terrane [*Liou et al.*, 1997; *Zhang et al.*, 2003; *Hacker et al.*, 2006; *Liu et al.*, 2006a, 2006b]. At the other end of the spectrum, smaller, thinner UHP units, such as the Kaghan Valley terrane [*Kaneko et al.*, 2003], that reached high temper-

atures and retained them through the bulk of the exhumation, probably followed a rapid subduction, rapid exhumation path, where the terranes spent minimal time at peak or near-peak metamorphic conditions.

6. Conclusions

[46] New high-precision Lu-Hf and Sm-Nd ages for (U)HP eclogites from the Western Gneiss Region of Norway from 413.9 ± 3.7 to 397.1 ± 4.8 Ma add to existing data that document a 20-Ma record of high-pressure metamorphism for an area spanning 60 × 220 km. These data require slow average subduction (∼2–4 mm a^{-1}) and rapid, near-isothermal exhumation (∼10–30 mm a^{-1}), followed by rapid cooling (15–50°C Ma^{-1}). Thermal models indicate that this *P-T-t* path is likely to have occurred at >7 km depth within a downgoing slab >30 km thick during subduction that initiated within a relatively warm continent. Other UHP terranes that show similar geochronologic and *P-T* characteristics, such as the Dabie-Sulu UHP terrane, may have developed in a similar manner.

[47] **Acknowledgments.** Samples of the Gossa eclogite were generously provided by K. Hollocher, P. Robinson, and E. Walsh, who collected the sample in 2004. The eclogite was discovered in 2000 by P. Robinson, and S. Cuthbert. R. Parrish offered an insightful review. Funding provided by NSF grant EAR-0510453 to B. R. Hacker.

References

Andersen, T. B., H. Austrheim, and E. A. J. Burke (1991), Mineral–fluid–melt interactions in high-pressure shear zones in the Bergen Arcs nappe complex, Caledonides of W. Norway: Implications for the fluid regime in Caledonian eclogite-facies metamorphism, *Lithos*, *27*, 187–204, doi:10.1016/0024-4937(91)90012-A.

Andersen, T. B., H. N. Berry, IV, D. R. Lux, and A. Andresen (1998), The tectonic significance of pre-Scandian $^{40}Ar/^{39}Ar$ phengite cooling ages from the Caledonides of western Norway, *J. Geol. Soc.*, *155*, 297–309, doi:10.1144/gsjgs.155.2.0297.

Blichert-Toft, J., and F. Albarede (1997), The Lu-Hf isotope geochemistry of chondrites and the evolution of the mantle-crust system, *Earth Planet. Sci. Lett.*, *148*(1–2), 243–258, doi:10.1016/S0012-821X(97)00040-X.

Carswell, D. A., and S. J. Cuthbert (2003), Ultrahigh pressure metamorphism in the Western Gneiss Region of Norway, in *Ultrahigh Pressure Metamorphism*, *EMU Notes Mineral.*, vol. 5, edited by D. A. Carswell and R. Compagnoni, pp. 51–73, Eur. Mineral. Union, Vienna, Austria.

Carswell, D. A., P. J. O′Brien, R. N. Wilson, and M. Zhai (1997), Thermobarometry of phengite-bearing eclogites in the Dabie Mountains of central China, *J. Metamorph. Geol.*, *15*, 239–252, doi:10.1111/j.1525-1314.1997.00014.x.

Carswell, D. A., H. K. Brueckner, S. J. Cuthbert, K. Mehta, and P. J. O′Brien (2003a), The timing of stabilisation and the exhumation rate for ultra-high pressure rocks in the Western Gneiss Region of Norway, *J. Metamorph. Geol.*, *21*, 601–612, doi:10.1046/j.1525-1314.2003.00467.x.

Carswell, D. A., R. D. Tucker, P. J. O'Brien, and T. E. Krogh (2003b), Coesite micro-inclusions and the U/Pb age of zircons from the Hareidland eclogite in the Western Gneiss Region of Norway, *Lithos*, *67*, 181–190, doi:10.1016/S0024-4937(03)00014-8.

Carswell, D. A., H. L. M. van Roermund, and D. F. Wiggers de Vries (2006), Scandian ultrahigh-pressure metamorphism of Proterozoic basement rocks on Fjortoft and Otroy, Western Gneiss Region, Norway, *Int. Geol. Rev.*, *48*, 957–977, doi:10.2747/0020-6814.48.11.957.

Chopin, C., C. Henry, and A. Michard (1991), Geology and petrology of the coesite-bearing terrain, Dora Maira massif, western Alps, *Eur. J. Mineral.*, *3*, 263–291.

Cohen, A. S., R. K. O′Nions, R. Siegenthaler, and W. L. Griffin (1988), Chronology of the pressure–temperature history recorded by a granulite terrain, *Contrib. Mineral. Petrol.*, *98*, 303–311, doi:10.1007/BF00375181.

Corfu, F. (1980), U-Pb and Rb-Sr systematics in a polyorogenic segment of the Precambrian shield, central southern Norway, *Lithos*, *13*, 305–323, doi:10.1016/0024-4937(80)90051-1.

Cuthbert, S. J., D. A. Carswell, E. J. Krogh-Ravna, and A. Wain (2000), Eclogites and eclogites in the Western Gneiss Region, Norwegian Caledonides, *Lithos*, *52*, 165–195, doi:10.1016/S0024-4937(99)00090-0.

Dobrzhinetskaya, L. F., E. A. Eide, R. B. Larsen, B. A. Sturt, R. G. Tronnes, D. C. Smith, W. R. Taylor, T. V. Posukhova, and T. V. Posukhova (1995), Microdiamond in high-grade metamorphic rocks of the Western Gneiss Region, Norway, *Geology*, *23*, 597–600, doi:10.1130/0091-7613(1995)023<0597:MIHGMR>2.3.CO;2.

Eide, E. A., M. O. McWilliams, and J. G. Liou (1994), $^{40}Ar/^{39}Ar$ geochronologic constraints on the exhumation of HP-UHP metamorphic rocks in east-central China, *Geology*, *22*, 601–604, doi:10.1130/0091-7613(1994)022<0601:AAGAEO>2.3.CO;2.

Ernst, W. G. (2006), Preservation/exhumation of ultra-high-pressure subduction complexes, *Lithos*, *92*, 321–335, doi:10.1016/j.lithos.2006.03.049.

Ernst, W. G., and S. M. Peacock (1996), A thermotectonic model for preservation of ultrahigh-pressure phases in metamorphosed continental crust, in *Subduction Top to Bottom*, *Geophys. Monogr. Ser.*, vol. 96, edited by G. E. Bebout et al., pp. 171–178, AGU, Washington, D. C.

Glodny, J., A. Kuehn, and H. Austrheim (2008), Diffusion versus recrystallization processes in Rb/Sr geochronology: Isotopic relics in eclogite facies rocks, Western Gneiss Region, Norway, *Geochim. Cosmochim. Acta*, *72*, 506–525, doi:10.1016/j.gca.2007.10.021.

Griffin, W. L., and H. K. Brueckner (1980), Caledonian Sm-Nd ages and a crustal origin for Norwegian eclogites, *Nature*, *285*, 319–321, doi:10.1038/285319a0.

Griffin, W. L., and H. K. Brueckner (1985), REE, Rb-Sr and Sm-Nd studies of Norwegian eclogites, *Chem. Geol.*, *52*, 249–271.

Griffin, W. L., H. Austrheim, K. Brastad, I. Bryhni, A. G. Krill, E. J. Krogh, M. B. E. Mørk, H. Qvale, and B. Torudbakken (1985), High-pressure metamorphism in the Scandinavian Caledonides, in *The Caledonide Orogen: Scandinavia and Related Areas*, vol. 2, edited by D. G. Gee and B. A. Sturt, pp. 783–801, John Wiley, Chichester, U.K.

Hacker, B. R. (1990), Simulation of the metamorphic and deformational history of the metamorphic sole of the Oman ophiolite, *J. Geophys. Res.*, *95*, 4895–4907, doi:10.1029/JB095iB04p04895.

Hacker, B. R. (2006), Pressures and temperatures of ultrahigh-pressure metamorphism: Implications for UHP tectonics and H2O in subducting slabs, *Int. Geol. Rev.*, *48*, 1053–1066.

Hacker, B. R. (2007), Ascent of the ultrahigh-pressure Western Gneiss Region, Norway, in *Convergent Margin Terranes and Associated Regions: A Tribute to W. G. Ernst*, edited by M. Cloos et al., *Spec. Pap. Geol. Soc. Am.*, *419*, 171–184.

Hacker, B. R., and P. B. Gans (2005), Continental collisions and the creation of ultrahigh-pressure terranes: Petrology and thermochronology of nappes in the central Scandinavian Caledonides, *Geol. Soc. Am. Bull.*, *117*, 117–134, doi:10.1130/B25549.1.

Hacker, B. R., L. Ratschbacher, L. E. Webb, T. R. Ireland, A. Calvert, S. Dong, H.-R. Wenk, and D. Chateigner (2000), Exhumation of ultrahigh-pressure continental crust in east-central China: Late Triassic–Early Jurassic tectonic unroofing, *J. Geophys. Res.*, *105*, 13,339–13,364, doi:10.1029/2000JB900039.

Hacker, B. R., A. T. Calvert, R. Y. Zhang, W. G. Ernst, and J. G. Liou (2003), Ultra-rapid exhumation of ultrahigh pressure diamond-bearing metasedimentary rocks of the Kokchetav Massif, Kazakhstan?, *Lithos*, *70*, 61–75, doi:10.1016/S0024-4937(03)00092-6.

Hacker, B. R., S. Wallis, L. Ratschbacher, M. Grove, and G. Gehrels (2006), High-temperature geochronology constraints on the tectonic history and architecture of the ultrahigh-pressure Dabie-Sulu Orogen, *Tectonics*, *25*, TC5006, doi:10.1029/2005TC001937.

Hirajima, T., and D. Nakamura (2003), The Dabie-Sulu orogen, in *Ultrahigh Pressure Metamorphism*, *EMU Notes Mineral.*, vol. 5, edited by D. A. Carswell and R. Compagnoni, pp. 105–144, Eur. Mineral. Union, Vienna, Austria.

Hollocher, K., P. Robinson, M. P. Terry, and E. Walsh (2007), Application of major- and trace-element geochemistry to refine U-Pb zircon, and Sm/Nd or Lu/Hf sampling targets for geochronology of HP and UHP eclogites, Western Gneiss Region, Norway, *Am. Mineral.*, *92*, 1919–1924, doi:10.2138/am.2007.2405.

Hurich, C. A. (1996), Kinematic evolution of the lower plate during intracontinental subduction: An example from the Scandinavian Caledonides, *Tectonics*, *15*, 1248–1263, doi:10.1029/96TC00828.

Jamtveit, B., D. A. Carswell, and E. W. Mearns (1991), Chronology of the high-pressure metamorphism of Norwegian garnet peridotites/pyroxenites, *J. Metamorph. Geol.*, *9*, 125–139, doi:10.1111/j.1525-1314.1991.tb00509.x.

Jarrard, R. D. (2003), Subduction fluxes of water, carbon dioxide, chlorine, and potassium, *Geochem. Geophys. Geosyst.*, *4*(5), 8905, doi:10.1029/2002GC000392.

Kaneko, Y., I. Katayama, H. Yamamoto, K. Misawa, M. Ishikawa, H. U. Rehman, A. B. Kausar, and

K. Shiraishi (2003), Timing of Himalayan ultra-high-pressure metamorphism: Sinking rate and subduction angle of the Indian continental crust beneath Asia, *J. Metamorph. Geol.*, *21*(6), 589–599, doi:10.1046/j.1525-1314.2003.00466.x.

Krogh, E. J. (1980), Geochemistry and petrology of glaucophane-bearing eclogites and associated rocks from Sunnfjord, western Norway, *Lithos*, *13*, 355–380, doi:10.1016/0024-4937(80)90054-7.

Krogh, E. J. (1982), Metamorphic evolution of Norwegian country-rock eclogites, as deduced from mineral inclusions and compositional zoning in garnets, *Lithos*, *15*, 305–321, doi:10.1016/0024-4937(82)90021-4.

Krogh, T., Y. Kwok, P. Robinson, and M. P. Terry (2004), U-Pb constraints on the subduction-extension interval in the Averøya-Nordøyane area, Western Gneiss Region, Norway, paper presented at Goldschmidt Conference, Eur. Assoc. for Geochem., Copenhagen, Denmark.

Krogh Ravn, E. J., and M. P. Terry (2004), Geothermobarometry of phengite-kyanite-quartz/coesite eclogites, *J. Metamorph. Geol.*, *22*, 579–592, doi:10.1111/j.1525-1314.2004.00534.x.

Kylander-Clark, A. R. C., B. R. Hacker, C. M. Johnson, B. L. Beard, N. J. Mahlen, and T. J. Lapen (2007), Coupled Lu-Hf and Sm-Nd geochronology constrains progade and exhumation histories of high- and ultrahigh-pressure eclogites from western Norway, *Chem. Geol.*, *242*, 137–154, doi:10.1016/j.chemgeo.2007.03.006.

Kylander-Clark, A., B. R. Hacker, and J. M. Mattinson (2008), Slow exhumation of UHP terranes: Titanite and rutile ages of the Western Gneiss Region, Norway, *Earth Planet. Sci. Lett.*, *272*, 531–540, doi:10.1016/j.epsl.2008.05.019.

Lallemand, S., A. Heuret, and D. Boutelier (2005), On the relationships between slab dip, back-arc stress, upper plate absolute motion, and crustal nature in subduction zones, *Geochem. Geophys. Geosyst.*, *6*, Q09006, doi:10.1029/2005GC000917.

Lapen, T. J., C. M. Johnson, L. P. Baumgartner, N. J. Mahlen, B. L. Beard, and J. M. Amato (2003), Burial rates during prograde metamorphism of an ultra-high-pressure terrane: An example from Lago di Cignana, western Alps, Italy, *Earth Planet. Sci. Lett.*, *215*, 57–72, doi:10.1016/S0012-821X(03)00455-2.

Lapen, T. J., N. J. Mahlen, C. M. Johnson, and B. L. Beard (2004), High precision Lu and Hf isotope analyses of both spiked and unspiked samples: A new approach, *Geochem. Geophys. Geosyst.*, *5*, Q01010, doi:10.1029/2003GC000582.

Leech, M. L., S. Singh, A. K. Jain, S. L. Klemperer, and R. M. Manickavasagam (2005), The onset of India-Asia continental collision; early, steep subduction required by the timing of UHP metamorphism in the western Himalaya, *Earth Planet. Sci. Lett.*, *234*, 83–97, doi:10.1016/j.epsl.2005.02.038.

Liou, J. G., R. Y. Zhang, and B. M. Jahn (1997), Petrology, geochemistry and isotope data on a ultrahigh-pressure jadeite quartzite from Shuanghe, Dabie Mountains, east-central China, *Lithos*, *41*, 59–78, doi:10.1016/S0024-4937(97)82005-1.

Liu, D., P. Jian, A. Kroener, and S. Xu (2006a), Dating of prograde metamorphic events deciphered from episodic zircon growth in rocks of the Dabie-Sulu UHP complex, China, *Earth Planet. Sci. Lett.*, *250*, 650–666, doi:10.1016/j.epsl.2006.07.043.

Liu, J., K. Ye, and M. Sun (2006b), Exhumation P-T path of UHP eclogites in the Hong'an area, western Dabie Mountains, China, *Lithos*, *89*, 154–173, doi:10.1016/j.lithos.2005.12.002.

Maruyama, S., and C. D. Parkinson (2000), Overview of the geology, petrology and tectonic framework of the high-pressure–ultrahigh-pressure metamorphic belt of the Kokchetav Massif, Kazakhstan, *Isl. Arc*, *9*, 439–455, doi:10.1046/j.1440-1738.2000.00288.x.

Masago, H. (2000), Metamorphic petrology of the Barchi-Kol metabasites, western Kokchetav ultra-high-pressure–high-pressure assif, northern Kazakhstan, *Isl. Arc*, *9*, 358–378, doi:10.1046/j.1440-1738.2000.00283.x.

Mattinson, C. G., J. L. Wooden, J. G. Liou, D. K. Bird, and C. Wu (2006), Age and duration of eclogite-facies metamorphism, north Qaidam HP/UHP terrane, western China, *Am. J. Sci.*, *306*, 683–711, doi:10.2475/09.2006.01.

McClelland, W. C., S. E. Power, J. A. Gilotti, F. K. Mazdab, and B. Wopenka (2006), U-Pb SHRIMP geochronology and trace-element geochemistry of coesite-bearing zircons, north-east Greenland Caledonides, in *Ultrahigh-Pressure Metamorphism: Deep Continental Subduction*, edited by B. R. Hacker, W. C. McClelland, and J. G. Liou, *Spec. Pap. Geol. Soc. Am.*, *403*, 23–42.

McKenzie, D., and R. K. O'Nions (1991), Partial melt distributions from inversion of rare earth element concentrations, *J. Petrol.*, *32*, 1021–1091.

Mearns, E. W. (1986), Sm-Nd ages for Norwegian garnet peridotite, *Lithos*, *19*, 269–278, doi:10.1016/0024-4937(86)90027-7.

Mørk, M. B. E., and E. W. Mearns (1986), Sm-Nd isotopic systematics of a gabbro-eclogite transition, *Lithos*, *19*, 255–267, doi:10.1016/0024-4937(86)90026-5.

Ota, T., M. Terabayashi, C. D. Parkinson, and H. Masago (2000), Thermobaric structure of the Kokchetav ultrahigh-pressure–high-pressure massif deduced from a north–south transect in the Kulet and Saldat-Kol regions, northern Kazakhstan, *Isl. Arc*, *9*, 328–357, doi:10.1046/j.1440-1738.2000.00282.x.

Parrish, R. R., S. J. Gough, M. P. Searle, and D. J. Waters (2006), Plate velocity exhumation of ultra-high-pressure eclogites in the Pakistan Himalaya, *Geology*, *34*, 989–992, doi:10.1130/G22796A.1.

Prince, C. I., J. Kosler, D. Vance, and D. Guenther (2000), Comparison of laser ablation ICP-MS and isotope dilution REE analyses—Implications for Sm-Nd garnet geochronology, *Chem. Geol.*, *168*, 255–274, doi:10.1016/S0009-2541(00)00203-5.

Reinecke, T. (1998), Prograde high- to ultrahigh-pressure metamorphism and exhumation of oceanic sediments at Lago di Cignana, Zermatt-Saas zone, Western Alps, *Lithos*, *42*, 147–189, doi:10.1016/S0024-4937(97)00041-8.

Roberts, D., and D. G. Gee (1985), An introduction to the structure of the Scandinavian Caledonides, in *The Caledonide Orogen–Scandinavia and Related Areas*, vol. 1, edited by D. G. Gee and B. A. Sturt, pp. 55–68, John Wiley, Chichester, U.K.

Røhr, T. S., F. Corfu, H. Austrheim, and T. B. Andersen (2004), Sveconorwegian U-Pb zircon and monazite ages of granulite-facies rocks, Hisarøya Gulen, Western Gneiss Region, Norway, Norwegian, *J. Geol.*, *84*, 251–256.

Root, D. B., B. R. Hacker, J. M. Mattinson, and J. L. Wooden (2004), Young age and rapid exhumation of Norwegian ultrahigh-pressure rocks: An ion microprobe and chemical abrasion study, *Earth Planet. Sci. Lett.*, *228*, 325–341, doi:10.1016/j.epsl.2004.10.019.

Root, D. B., B. R. Hacker, P. B. Gans, M. N. Ducea, E. A. Eide, and J. L. Mosenfelder (2005), Discrete ultrahigh-pressure domains in the Western Gneiss region, Norway; implications for formation and exhumation, *J. Metamorph. Geol.*, *23*, 45–61, doi:10.1111/j.1525-1314.2005.00561.x.

Roselle, G. T., and M. Engi (2002), Ultra high pressure (UHP) terrains: Lessons from thermal modeling, *Am. J. Sci.*, *302*, 410–441, doi:10.2475/ajs.302.5.410.

Rubatto, D., and J. Hermann (2001), Exhumation as fast as subduction?, *Geology*, *29*, 3–6, doi:10.1130/0091-7613(2001)029<0003:EAFAS>2.0.CO;2.

Rudnick, R., and S. Gao (2003), The composition of the continental crust, in *Treatise on Geochemistry*, vol. 3, *The Crust*, edited by R. L. Rudnick, pp. 1–64, Elsevier, Amsterdam, doi:10.1016/B0-08-043751-6/03016-4.

Schärer, U. (1980), U-Pb and Rb-Sr dating of a polymetamorphic nappe terrain: The Caledonian Jotun Nappe, southern Norway, *Earth Planet. Sci. Lett.*, *49*, 205–218, doi:10.1016/0012-821X(80)90065-5.

Schärer, U., and L. Labrousse (2003), Dating the exhumation of UHP rocks and associated crustal melting in the Norwegian Caledonides, *Contrib. Mineral. Petrol.*, *144*, 758–770, doi:10.1007/s00410-002-0428-8.

Scherer, E., C. Münker, and K. Mezger (2001), Calibration of the lutetium-hafnium clock, *Science*, *293*, 683–686, doi:10.1126/science.1061372.

Schertl, H. P., W. Schreyer, and C. Chopin (1991), The pyrope-cœsite rocks and their country rocks at Parigi, Dora-Maira Massif, Western Alps: Detailed petrography, mineral chemistry and PT-path, *Contrib. Mineral. Petrol.*, *108*, 1–21, doi:10.1007/BF00307322.

Skora, S., L. P. Baumgartner, N. J. Mahlen, C. M. Johnson, S. Pilet, and E. Hellebrand (2006), Diffusion-limited REE uptake by eclogite garnets and its consequences for Lu-Hf and Sm-Nd geochronology, *Contrib. Mineral. Petrol.*, *152*, 703–720, doi:10.1007/s00410-006-0128-x.

Terry, M. P., and P. Robinson (2003), Evolution of amphibolite-facies structural features and boundary conditions for deformation during exhumation of high- and ultrahigh-pressure rocks, Nordøyane, Western Gneiss Region, Norway, *Tectonics*, *22*(4), 1036, doi:10.1029/2001TC001349.

Terry, M. P., and P. Robinson (2004), Geometry of eclogite-facies structural features: Implications for production and exhumation of ultrahigh-pressure and high-pressure rocks, Western Gneiss Region, Norway, *Tectonics*, *23*, TC2001, doi:10.1029/2002TC001401.

Terry, M. P., P. Robinson, M. A. Hamilton, and M. J. Jercinovic (2000a), Monazite geochronology of UHP and HP metamorphism, deformation, and exhumation, Nordøyane, Western Gneiss Region, Norway, *Am. Mineral.*, *85*, 1651–1664.

Terry, M. P., P. Robinson, and E. J. K. Ravna (2000b), Kyanite eclogite thermobarometry and evidence for thrusting of UHP over HP metamorphic rocks, Nordøyane, Western Gneiss Region, Norway, *Am. Mineral.*, *85*, 1637–1650.

Tucker, R. D., R. Boyd, and S.-J. Barnes (1990), A U-Pb zircon age for the Råna intrusion, N Norway: New evidence of basic magmatism in the Scandinavian Caledonides in Early Silurian time, *Nor. Geol. Tidsskr.*, *70*, 229–239.

Tucker, R. D., P. Robinson, A. Solli, D. G. Gee, T. Thorsnes, T. E. Krogh, Ø. Nordgulen, and M. E. Bickford (2004), Thrusting and extension in the Scandian hinterland, Norway: New U-Pb ages and tectonostratigraphic evidence, *Am. J. Sci.*, *304*, 477–532, doi:10.2475/ajs.304.6.477.

Turcotte, D. L., and G. Schubert (2002), *Geodynamics*, Cambridge Univ. Press, Cambridge, U.K.

van Keken, P. E., B. Kiefer, and S. M. Peacock (2002), High-resolution models of subduction zones: Implications for mineral dehydration reactions and the transport of water into the deep mantle, *Geochem. Geophys. Geosyst.*, *3*(10), 1056, doi:10.1029/2001GC000256.

van Roermund, H. L., and M. R. Drury (1998), Ultra-high pressure (P > 6 GPa) garnet peridotites in western Norway: Exhumation of mantle rocks from >185 km depth, *Terra Nova*, *10*, 295–301, doi:10.1046/j.1365-3121.1998.00213.x.

van Roermund, H. L. M., M. R. Drury, A. Barnhoorn, and A. de Ronde (2001), Relict majoritic garnet microstructures from ultra-deep orogenic peridotites in western Norway, *J. Petrol.*, *42*, 117–130, doi:10.1093/petrology/42.1.117.

Wain, A., D. Waters, and H. Austrheim (2001), Metastability of granulites and processes of eclogitization in the UHP region of western Norway, *J. Metamorph. Geol.*, *19*, 609–625, doi:10.1046/j.0263-4929.2001.00333.x.

Walsh, E. O. (2003), Exhumation of the ultrahigh-pressure/high-pressure terrane of the Western Gneiss region, Norway, Ph.D. dissertation thesis, 119 pp., Univ. of Calif, Santa Barbara.

Walsh, E. O., and B. R. Hacker (2004), The fate of subducted continental margins: Two-stage exhumation of the high-pressure to ultrahigh-pressure Western Gneiss complex, Norway, *J. Metamorph. Geol.*, *22*, 671–689, doi:10.1111/j.1525-1314.2004.00541.x.

Walsh, E. O., B. R. Hacker, P. B. Gans, M. Grove, and G. E. Gehrels (2007), Protolith ages and exhumation histories of (ultra)high-pressure rocks across the Western Gneiss Region, Norway, *Geol. Soc. Am. Bull.*, *119*, 289–301, doi:10.1130/B25817.1.

Warren, C. J., C. Beaumont, and R. A. Jamieson (2008), Modelling tectonic styles and ultra-high pressure (UHP) rock exhumation during the transition from oceanic subduction to continental collision, *Earth Planet. Sci. Lett.*, *267*, 129–145, doi:10.1016/j.epsl.2007.11.025.

Young, D. (2005), Amphibolite to ultrahigh-pressure transition in western Norway, Ph.D. dissertation thesis, Univ. of Calif., Santa Barbara.

Young, D. J., B. R. Hacker, T. B. Andersen, F. Corfu, G. E. Gehrels, and M. Grove (2007a), Amphibolite to ultrahigh-pressure transition in western Norway: Implications for exhumation tectonics, *Tectonics*, *26*, TC1007, doi:10.1029/2004TC001781.

Young, D. J., B. R. Hacker, T. B. Andersen, and F. Corfu (2007b), Prograde amphibolite facies to ultrahigh-pressure transition along Nordfjord, western Norway: Implications for exhumation tectonics, *Tectonics*, *26*, TC1007, doi:10.1029/2004TC001781.

Zhang, R. Y., J. G. Liou, Y. F. Zheng, and B. Fu (2003), Transition of UHP eclogites to gneissic rocks of low-amphibolite facies during exhumation: Evidence from the Dabie terrane, central China, *Lithos*, *70*, 269–291, doi:10.1016/S0024-4937(03)00102-6.

Zheng, Y., B. Fu, B. Gong, and L. Li (2003), Stable isotope geochemistry of ultrahigh pressure metamorphic rocks from the Dabie-Sulu Orogen in China: Implications for geodynamics and fluid regime, *Earth Sci. Rev.*, *62*, 105–161, doi:10.1016/S0012-8252(02)00133-2.

B. L. Beard, C. M. Johnson, and N. J. Mahlen, Department of Geology and Geophysics, University of Wisconsin-Madison, Madison, WI 53706, USA.

B. R. Hacker and A. R. C. Kylander-Clark, Department of Earth Science, University of California, Building 526, Santa Barbara, CA 93106, USA. (kylander@geol.ucsb.edu)